



DFT quantum chemical calculations (Fukui functions, NLO, TDOS, OPDOS, DNA/ECT) on 4-(dec-2yn-1-yloxy)phthalonitrile

Serap Uzun

Department of Basic Sciences, Faculty of Engineering, Samsun University, Samsun, Turkey

E-mail: serap.uzun@samsun.edu.tr

Received 12 November 2020; accepted (revised) 28 June 2022

In this study, structural and electronic properties of 4-(dec-2yn-1-yloxy)phthalonitrile are analyzed theoretically. The optimized structure in the gas phase of the title compound is achieved by density functional theory method with the B3LYP hybrid functional using 6-31G (d,p) basis set. Then, IR, $^1\text{H-NMR}$, $^{13}\text{C-NMR}$ spectroscopic properties of the title molecule are calculated and compared with the corresponding experimentally ones. Besides these, the molecular electrostatic potential surface, frontier molecular orbitals, chemical activity, Fukui function analysis, nonlinear optical properties (NLO) in different solvent environments, total, partial and overlap population density of state diagrams are derived. Finally, the interactions between the title molecule with adenine, cytosine, thymine and guanine which are DNA bases are investigated by using the electrophilicity-based charge transfer method and charge transfer. According to NLO calculations, the value of the first hyperpolarizability of the title compound in the gas phase is found nearly twenty two times more than that of urea.

Keywords: Phthalonitrile, DFT, NLO, OPDOS, ECT

Phthalonitriles and its derivatives are an important class of molecules with a wide range of applications such as sensors, catalysis, non-linear optics (NLO), optical data storage, photodynamic cancer therapy and nanotechnology^{1,2}. The polymers of phthalonitrile are also an important class of high performance polymers, which are easily processable, and display good mechanical properties, outstanding thermal and thermal-oxidative stability³.

In previous publication, synthesis, IR, UV-visible, $^1\text{H-NMR}$, $^{13}\text{C-NMR}$, mass (MALDI-TOF technique) spectroscopic data and elemental analysis of the title molecule (Fig. 1) had been studied and interpreted⁴. To the best of my knowledge, the theoretical calculations of molecular structure and electronic properties for the title molecule have not been investigated until now. The aim of this study is to investigate the energetic and structural properties of 4-(dec-2yn-1-yloxy)phthalonitrile via density functional theory (DFT) calculations which are the most commonly used method in recent years because it gives results that are close to the experimental ones.

In this study, the optimized molecular geometry in gas phase, molecular electrostatic potential (MEP) map, frontier molecular orbitals (FMOs) and chemical activity, total, partial and overlap population density of states, Fukui functions, the solvent effect on the

nonlinear optical (NLO) behaviour of the title molecule were computed using B3LYP/DFT. Furthermore, the charge exchange between the title molecule and some DNA bases was examined. In addition to these theoretical calculations, IR, $^1\text{H-NMR}$, $^{13}\text{C-NMR}$ spectroscopic properties of the title molecule have also been studied theoretically and compared with the experimentally ones. This study is important in terms of containing some information that researchers interested in phthalonitrile may be obtained without conducting costly experiments.

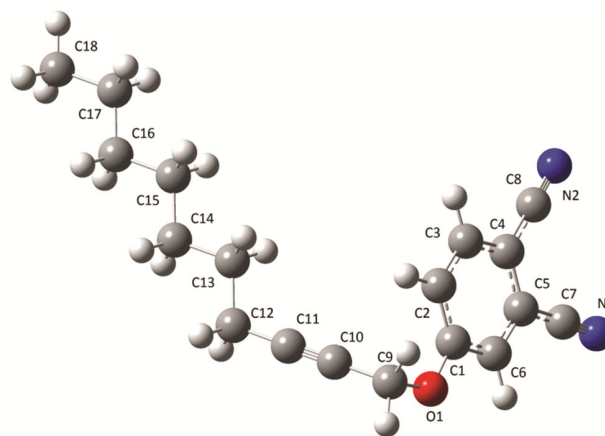


Fig. 1 — Theoretical geometric structure of 4-(dec-2yn-1-yloxy)phthalonitrile (with B3LYP/6-31G(d,p) level)

Computational procedures

All of the quantum chemical calculations were performed on a personal computer by using Gaussian 03W⁵ program package together with B3LYP/6-31G(d,p) level of the Density functional theory method^{6,7}. With using Gaussview visualization program⁸, the manually drawn geometry was selected as the initial geometry for geometry optimization. The harmonic vibrational modes for optimized molecule were calculated were scaled by 0.9627 [Ref.9]. As a result of the calculations, no imaginary frequency is observed, indicating that the structure was in stationary point. The ¹H and ¹³C-NMR isotropic shielding were calculated with the GIAO method^{10,11} using the optimized parameters obtained from DFT calculations. To evaluate the NLO behaviour of the title molecule in the solvent media, the PCM (polarizable continuum model)¹⁰ was used with B3LYP/6-31G(d,p). To obtain density of states (TDOS or DOS), the partial density of states (PDOS) and overlap population density of states (OPDOS or COOP) spectra, GaussSum 2.2 program was used¹³.

Results and Discussion

IR analysis

The vibrational modes of the molecule were calculated by using B3LYP/6-31G(d,p) method. Due to the values of all frequencies were positive it was understood that the minimum energy conformation of the molecule was reached for this study. It is known that the systematic errors occur in the calculated harmonic vibrational frequencies when it is compared with experimental vibrational frequencies¹⁴. Since quantum mechanical calculations neglect the anharmonicity all the calculated frequencies were scaled by 0.9627 for B3LYP/6-31G(d,p). The DFT calculations calculate vibrational frequencies without taking into account the anharmonic effect, so there may be some differences between the theoretical and experimental frequencies¹⁵. Despite the differences observed in the frequencies, it can be generally said that the theoretically calculated frequencies support their experimentally obtained values.

Table 1 summarizes the experimental and calculated vibrational frequencies and their assignments. In the experimental IR data of the molecule C≡N stretching vibration was observed at 2231 cm⁻¹ [Ref. 4] that have been calculated with B3LYP/6-31G(d,p) at 2260, 2267 for phthalonitrile group and 2272 cm⁻¹, for the other one, respectively.

While the stretching vibrations at 3086 and 3046 cm⁻¹ for aromatic CH groups, at 2922–2855 cm⁻¹ for aliphatic CH groups appeared experimentally⁴, the same modes theoretically appeared at 3119 and 3096 cm⁻¹ and at 2996–2898 cm⁻¹ for aromatic CH groups and for aliphatic CH groups, respectively.

NMR analysis

In previous publication, ¹H-NMR and ¹³C-NMR of the title molecule were studied experimentally by Saka and Caglar⁴. In this paper, to compare with the experimental chemical shift results, ¹H and ¹³C chemical shifts for the title molecule computed using GIAO method in chloroform at the B3LYP/6-31G(d,p) level. The experimental and computed ¹H and ¹³C chemical shifts were tabulated in Table 2. In the ¹H-NMR spectra of the title compound, the aromatic protons were obtained at 7.90 (d), 7.45 (m), 7.0 (d) ppm as experimentally⁴ while they were computed in the region 8.04, 7.58, 7.51 ppm. The aliphatic protons had shown signals at 4.79 (d), 2.20–2.14 (t), 1.48–1.33 (m), 0.90–0.81 (t) ppm as experimentally⁴ and the same signals at 4.90, 1.38, 2.23–1.31 ppm, respectively, as theoretically.

The NMR chemical shift signals for carbon atoms in the title molecule were observed at the interval of 161.88–14.83 ppm⁴ and they were calculated in the region of 155.46 –15.98 ppm. The nitrile carbon atoms for the title molecule were also observed at 117.30 and 112.54 ppm⁴, experimentally, while their computed values were obtained at 81.79 and 109.51 ppm, respectively. As a result of the calculations, it was seen that theoretical and experimental ¹H and ¹³C spectral values are matching.

Mulliken atomic charges (MPA)

The calculation of atomic charges is important to describe the electronic nature of the molecular systems¹⁶. In MPA, the total charges are equally divided between the participating atoms. MPA is mostly preferred because of its ease of use although it has shortcomings such as neglecting some elements to

Table 1 — Some experimental and calculated IR frequencies of the title molecule

Assignment	Experimental (cm ⁻¹) ⁴	Calculated (cm ⁻¹)
(Ar-H) str.	3086, 3046	3096–3119
(Aliph. C-H) str.	2922–2855	2898– 2996
C≡N str.	2231	2260, 2267
C≡C str.	–	2272
C-O str.	1667–1596	1480

str.: stretching

Table 2 — The experimental and computed ^1H and ^{13}C chemical shifts

Atom	Exp. ppm ⁴	Calc. ppm	Atom	Exp. ppm ⁴	Calc. ppm
C1	161.88	155.46	H2	7.90	8.04
C2	122.70	120.78			
C3	135.22	114.77	H3	7.45	7.58
C4	106.46	104.65			
C5	120.43	132.89			
C6	122.38	112.60	H6	7.00	7.51
C7	117.30	81.79			
C8	112.54	109.51			
C9	56.96	56.20	H9	4.79	4.90
C10	76.81	67.44			
C11	88.64	87.21			
C12	19.08	20.98	H12		2.23
C13	29.12	32.84	H13		1.48
C14	29.85	33.03	H14	1.48–1.33	1.26
C15	30.04	33.32	H15		1.30
C16	32.10	34.85	H16		1.31
C17	22.90	26.40	H17	2.20–2.14	1.38
C18	14.83	15.98	H18	0.90–0.81	0.92

Table 3 — Atomic Charges (MPA) of the title compound

Atom	MPA	Atom	MPA
C1	0.373332	C12	-0.305400
C2	-0.117828	C13	-0.183391
C3	-0.110128	C14	-0.176376
C4	0.137332	C15	-0.181308
C5	0.138863	C16	-0.170577
C6	-0.133068	C17	-0.177936
C7	0.251791	C18	-0.322362
C8	0.238972	O1	-0.521349
C9	-0.095902	N1	-0.525155
C10	-0.052156	N2	-0.517728
C11	0.082838		

be more electronegative¹⁷. The obtained results of MPA are presented in Table 3. When looking at the Table 3, it is clear that the most electronegative atoms are N1, N2 and O1 atoms. These results are consistent with MEP surface of the title molecule.

Frontier molecular orbitals and chemical activity

The frontier molecular orbitals (FMOs) have an important role to understand the nature of the electronic and optical properties, chemical reactions¹⁸. A low kinetic stability for a molecule requires having a narrow HOMO-LUMO energy gap, because as the electrons easily reach from HOMO to LUMO, the stability of the molecule decreases¹⁹⁻²¹. Fig. 2 shows the distributions and energy levels of the FMOs computed at the 6-31G(d,p) level for the title molecule. According to the investigation on the FMOs, the title compound has 75 occupied MOs. Both the HOMO and LUMO are localized on the ring to which the cyano groups are attached. As can be seen from Fig. 2, FMOs of the molecule are mostly π -antibonding type orbitals and the energy gap between them is 4.966 eV in gas

phase. This large energy gap emphasizes that the title compound has a good stability and a high chemical hardness as in previous studies²²⁻²⁴.

The values of hardness, softness, electronic chemical potential, Mulliken electronegativity and electrophilicity index for the title compound were calculated as described in a previous study²⁵ and values obtained in gas phase were 4.966 eV, 0.101 eV, -4.452 eV, 4.452 eV and 1.995 eV, respectively.

Total, partial, and overlap population density-of-states

The TDOS (total electronic density of states) (or DOS) plot is the presentation of molecular orbital (MO) and their contribution to chemical bonding through the OPDOS (overlap population electronic density of states) (or COOP) plot. So, the TDOS plot shows that the results of overlapping population in MO. The OPDOS (or COOP) diagrams show that the bonding, anti-bonding and nonbonding natures of the interaction of the two orbitals, atoms or groups. The value may be positive, negative or zero, the OPDOS diagrams indicate a bonding interaction because of the positive overlap population, an anti-bonding interaction due to negative overlap population and non-bonding interactions, respectively^{26,27}. Furthermore, the determination and comparison of the donor-acceptor properties of the ligands ascertained the bonding, non-bonding made by OPDOS diagrams. TDOS, PDOS and OPDOS diagrams of the title compound calculated by Mulliken population analysis are shown in the Figs. 3–5, respectively, with Gaussian curves of unit height and Full width at half maximum (FWHM) of

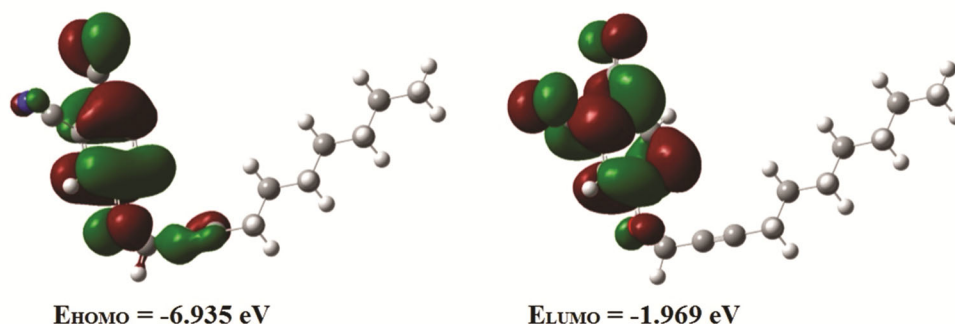


Fig. 2 – Molecular orbital surfaces for the HOMO and LUMO of the title compound

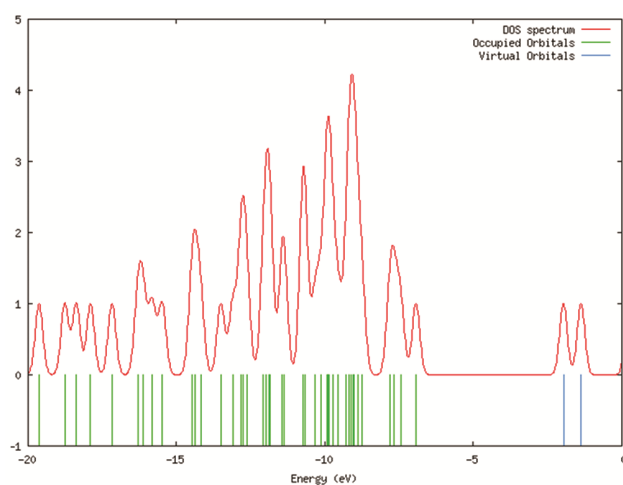


Fig. 3 — Calculated TDOS spectrum of the title compound

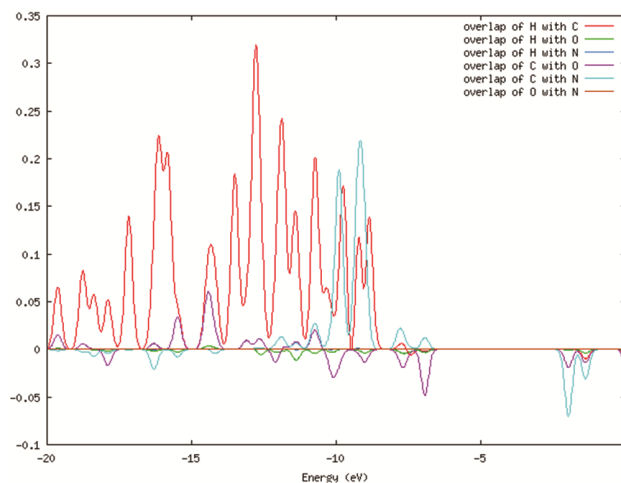


Fig. 5 — OPDOS (or COOP) spectrum for the title compound

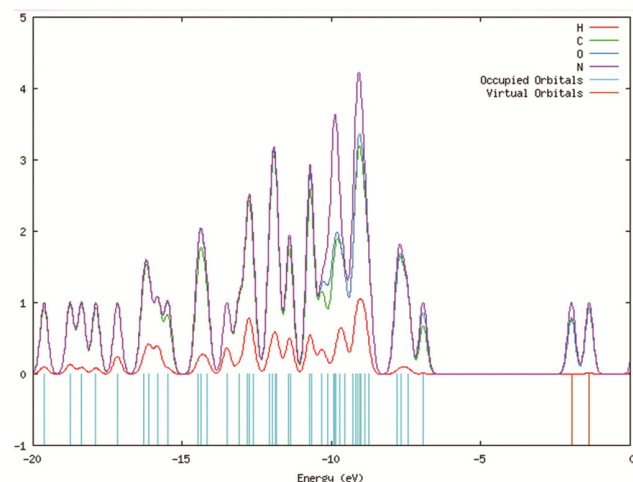


Fig. 4 — Calculated PDOS spectrum of the title compound

0.3 eV using GaussSum 2.2 program²⁸. From the Figs. 3–5, it can possible to obtain information that HOMO and LUMO energy construction and atoms energy distribution (C, O, N, H) and also defined the bonding character of the title compound according to TDOS, PDOS and OPDOS spectra, respectively. As a results

of analysis, HOMO orbitals are localized on the H, C, O and N atoms their contributions about 1%, 67%, 18%, 14%, respectively. Similarly, the LUMO orbitals are localized with 0%, 77%, 2%, 21% contribution on the H, C, O and N atoms, respectively. The least contribution comes from hydrogen atoms. Furthermore, when the OPDOS diagram (Fig. 5) is examined, it is clearly seen that between the H and C atoms (red line) is bonding interaction (positive) while there is nonbonding interaction (zero) between the O and N atoms (orange line).

Molecular electrostatic potential (MEP) surface

The MEP surface defines the energy of interaction with the molecule of a positive test charge. The colour of the surface in a given region depends upon whether the positive (blue) contribution of nuclei or the negative (red) one of electrons is dominant there^{28,29}. The negative and the positive regions on the MEP were related to electrophilic reactivity and nucleophilic reactivity, respectively. The molecular electrostatic potential (MEP) of the optimized

geometry was calculated at the B3LYP/6-31G(d,p) and demonstrated in Fig. 6(a). As easily can be seen from this figure, there are two negative regions mainly over the N1 and N2 atoms with values around -0.0664 and -0.0653 a.u., respectively. So, these are the most preferred sites for any electrophilic attack on the whole molecule. The maximum positive regions for the possible nucleophilic attack are localized on H atoms. Additionally, the electrostatic potential contour map for investigated molecule was shown in Fig. 6(b). Fig. 6 provides information on the regions where the molecule can interact intramolecularly.

The solvent effect on the nonlinear optical properties

The charge asymmetry of the molecule is disturbed by the effect of external electric field on the molecule and the non-linear optical properties become dominant. The charge asymmetry can also be disturbed by adding donor-acceptor groups to end of the molecule and so the polarizability and first order hyperpolarizability of the molecule is thus increased³⁰.

To investigated the effect of the solvent on the electronic charge distribution, the NLO properties of the title compound were calculated at B3LYP/6-31G(d,p) level with polarizable continuum model

(PCM)¹⁰. The dipole moments, polarizabilities and the first order hyperpolarizabilities, the energy gaps between the HOMO and LUMO in different solvents (CCl₄, chloroform, asetone, asetonitrile, DMSO, water) of the title molecule are tabulated in Table 4. As can be seen from the Table 4, because of the inductive solvent polarization effects in the polar solvents with the rising polarity of the solvent, the dipole moment increases. On the other hand, while the energy gap between the HOMO and LUMO decreases the first order hyperpolarizability of the title compound increases with increasing polarity of the solvent. As the HOMO-LUMO energy gap decreases, the electronic charge asymmetry of the molecule can be easily changed when the external electric field is applied. And so, the stability of the title compound decreases in going to the solution phase. In the gas phase, the calculated values of dipole moment, μ , polarizability, α , and the first hyperpolarizability, β for the title molecule are, 9.765 Debye, 30.553 Å³ and 8.628×10^{-30} cm⁵/esu, respectively. The value of the first hyperpolarizability of the title compound in the gas phase is found nearly twenty two times more than that of urea ($3.850676203 \times 10^{-31}$ cm⁵/esu) by using the same method³². So it can be said that the title molecule may be a good candidate to be NLO material.

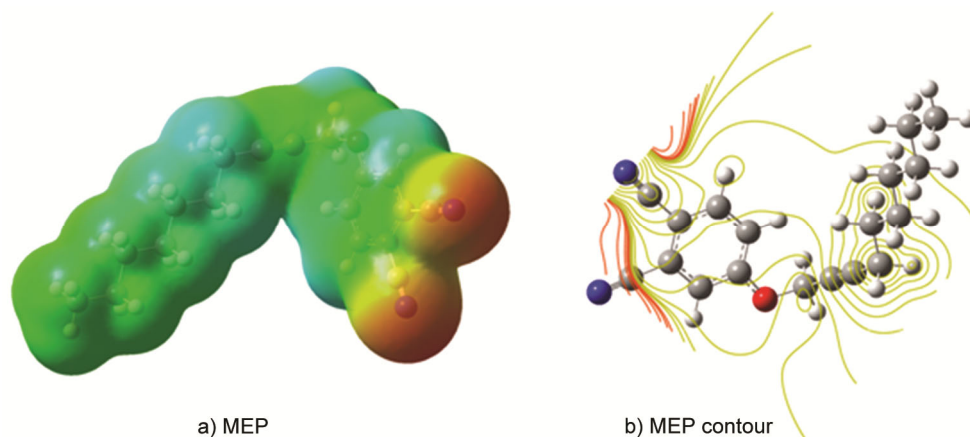


Fig. 6 — (a) MEP surface and (b) MEP contour for positive and negative potentials [density lie within a specific range at (000)] of the title compound

Table 4 — Theoretical energies (E), dipole moments (μ), molecular polarizabilities (α) and hyperpolarizability (β) in different media of the title compound

Medium	E (eV)	μ (D)	α (Å ³)	β ($\times 10^{-30}$ esu)	$E_{\text{HOMO-LUMO}}$
Gas ($\epsilon=1$)	-24017.657	9.765	30.553	8.628	4.9664
CCl ₄ ($\epsilon=2.228$)	-24017.830	10.673	34.896	8.722	4.9497
Chloroform ($\epsilon=4.9$)	-24017.967	11.351	37.373	11.989	4.9179
Asetone ($\epsilon=20.7$)	-24018.062	11.845	39.188	15.024	4.8913
Asetonitrile ($\epsilon=36.64$)	-24018.077	11.918	39.474	15.583	4.8880
DMSO ($\epsilon=46.7$)	-24018.079	11.933	39.523	15.677	4.8866
Water ($\epsilon=78.39$)	-24018.096	11.980	39.745	15.874	4.8864

Local reactivity descriptors

The Fukui function is one of the local reactivity determinants. Fukui functions are calculated with the basis of B3LYP/6-31G(d,p) level of theory, using the procedure given in previous studies^{25, 32, 33}. As a result of the calculations, N1, N2 and O1 atoms are the most susceptible sites for electrophilic attack in the title molecule (Table 5). Finally, it is seen that the Fukui function analysis and MEP results are in agreement with each other.

Electrophilicity-based charge transfer with DNA bases

The method of the electrophilicity based charge transfer (ECT) is important to investigate the relationship between molecules and DNA bases showing nucleophilic or electrophilic behaviour. The charges flow from the base to the functional group occurs when the ECT is greater than zero. If the ECT is less than zero, the charges flow occurs in the opposite direction³⁴⁻³⁶. For calculation ECT the ionization potential (IP) and electron affinity (EA) which were obtained from the energy of neutral, anionic and cationic species at the geometry of corresponding N electron neutral species are used. They are defined as follows:

$$IP = [E(N - 1) - E(N)] \quad \dots (1)$$

$$EA = [E(N) - E(N + 1)] \quad \dots (2)$$

The new reactivity index measures the stabilization in energy when the system reserves additional electronic charge (ΔN). The electronic chemical potential of a molecule determines the direction of charge transfer. While a reaction takes place between two molecules, species can act as an electrophile which has a higher value of electrophilicity index. Looking at the electrophilic index values, it can be seen that the adenine, guanine, cytosine and thymine from DNA basis are good nucleophiles so that they can attack the title molecule. Where ECT is explained as the difference between ΔN_{max} values of interacting molecules and is calculated by the following equation:

$$ECT = (\Delta N_{max})_A - (\Delta N_{max})_B \quad \dots (3)$$

$$(\Delta N_{max})_A = \mu_A/\eta_A \text{ and } (\Delta N_{max})_B = \mu_B/\eta_B \quad \dots (4)$$

The ECT values were calculated as 0.9569, 1.0632, 1.0213, 0.3379 for the adenine, guanine, cytosine and thymine, respectively. For the title molecule and DNA basis, the $IP, EA, \mu, \eta, \Delta N_{max}$ and ECT values were listed in Table 6. As can be seen from the Table 6,

Table 5 — Values of the Fukui function considering natural population analysis

Atom	q_j^-	q_j^+	q_j^0	f_j^-	f_j^+	f_j^0	$\Delta f(r)$
C1	0.27509	0.42616	0.34921	0.07412	0.07695	0.07553	0.00283
C2	-0.39460	-0.22411	-0.29210	0.10250	0.06799	0.17049	-0.03451
C3	-0.17405	-0.15198	-0.16408	0.00997	0.01210	0.02207	0.00213
C4	-0.25900	-0.00780	-0.16255	0.09645	0.15470	0.25120	0.05825
C5	-0.24750	-0.10000	-0.12055	0.12700	0.02055	0.14750	-0.10645
C6	-0.27016	-0.14431	-0.22142	0.04874	0.07712	0.12585	0.02838
C7	0.27226	0.28991	0.30967	0.03741	-0.01976	0.00882	-0.05717
C8	0.28879	0.29129	0.30667	0.01797	-0.01538	-0.01667	-0.03335
C9	-0.17762	-0.19604	-0.18117	-0.00355	-0.01487	-0.00921	-0.01132
C10	-0.08611	-0.08565	-0.10675	-0.02064	0.02110	0.00023	0.04174
C11	0.01428	0.13185	0.04267	0.02839	0.08918	0.05878	0.06079
C12	-0.53117	-0.54778	-0.53590	-0.00473	-0.01188	-0.00830	-0.00715
C13	-0.44680	-0.44573	-0.44647	-0.00033	0.00074	0.00053	0.00107
C14	-0.46207	-0.46289	-0.46259	-0.00052	-0.00030	-0.00041	0.00022
C15	-0.45785	-0.45778	-0.45778	0.00007	0.00000	0.00003	-0.00007
C16	-0.45983	-0.46040	-0.46024	-0.00041	-0.00016	-0.00028	0.00025
C17	-0.45994	-0.46005	-0.46002	-0.00008	-0.00003	-0.00005	0.00005
C18	-0.68560	-0.68643	-0.68601	-0.00041	-0.00042	0.00041	-0.00001
O1	-0.50733	-0.74464	-0.58448	-0.07715	-0.16016	0.11865	-0.08301
N1	-0.04085	-0.25845	-0.11561	-0.07476	-0.14284	-0.10880	-0.06808
N2	-0.41390	-0.20939	-0.27367	0.14023	0.06428	0.10225	-0.07595

Table 6 — The calculated IP, EA, μ , η , ΔN_{max} and ECT values for title compound

Compound & DNA Bases	IP (eV)	EA (eV)	μ (eV)	η (eV)	ΔN_{max}
Title Compound	-1.7123	-7.1668	4.4395	2.7272	1.6279
Adenine ECT=0.9569	-1.5696	7.9730	-3.2017	-4.7713	0.6710
Guanine ECT=1.0632	-2.0952	7.5307	-2.7178	-4.8129	0.5647
Cytosine ECT=1.0213	-1.4326	5.8498	-2.2086	-3.6412	0.6066
Thymine ECT= 0.3379	1.2099	9.5563	-5.3831	-4.1732	1.2899

while the DNA bases treated as electron acceptor, the title molecule treated as the electron donor for adenine, guanine, cytosine and thymine.

Conclusion

In the present work, both structural and electronic properties and harmonic vibrational frequencies, ^1H and ^{13}C -NMR isotropic shielding values of 4-(dec-2yn-1-yloxy)phthalonitrile were analyzed to using DFT/B3LYP/6-31G(d,p) method, theoretically. Generally, it can be said that experimental and theoretical spectroscopic data are in harmony, apart from minor differences due to neglected steric effects in theoretical calculations. The Mulliken atomic charges and detailed chemical activity calculations were made. MEP surface showed that the negative potential sites (electrophilic attack) are on the O and N atoms. This finding is in agreement with the Mulliken population analysis of the title compound. The contributions of molecular orbitals were analyzed by using total, partial and overlap populations density of states. The contribution of the atoms (H, C, O and N, respectively) in the title molecule to frontier molecular orbitals was calculated as 1%, 67%, 18%, 14% for HOMO and 0%, 77%, 2%, 21% for LUMO. NLO properties were investigated for six different solvents using PCM. As a result of calculations, the value of the first hyperpolarizability of the title molecule in the gas phase was found nearly 22 times more than that of urea. This results is indicate that the title molecule may be a good candidate to be NLO material. As a result of ECT, DNA bases showed nucleophilic nature, while title molecule displayed electrophilic nature. This ECT study shows that DNA bases have a significant effect on the relative stability and the hyperpolarizability of the title molecule. Calculated ECT values, it can be said that the molecule interact more with guanine. Finally, according to the calculated ECT values, it would not be wrong to say that the highest contribution to hyperpolarizability of the title compound comes from guanine base.

References

- Leznoff C C, Lever A B P, (Eds.), *Phthalocyanines: Properties and Applications*, Vols. 1-4, (VCH, New York) 1993.
- Kadish K M, Smith K M & Guillard R, (Eds.), *The Porphyrin Handbook*, (Academis Press, California) 2003.
- Çoruh A, Yılmaz F, Sengez B, Kurt M, Çınar M & Karabacak M, *Struct Chem*, 22 (2011) 45.
- Saka E T & Çağlar Y, *Catal Lett*, 147 (2017) 1471.
- Frisch M J, Trucks G W, Schlegel H B, Scuseria G E, Robb M A, Cheeseman J R, Montgomery J A, Vreven Jr T, Kudin K N, Burant J C, Millam J M, Iyengar S S, Tomasi J, Barone V, Mennucci B, Cossi M, Scalmani G, Rega N, Petersson G A, Nakatsuji H, Hada M, Ehara M, Toyota K, Fukuda R, Hasegawa J, Ishida M, Nakajima T, Honda Y, Kitao O, Nakai H, Klene M, Li X, Knox J E, Hratchian H P, Cross J B, Adamo C, Jaramillo J, Gomperts R, Startmann R E, Yazyev O, Austin A J, Cammi R, Pomelli C, Ochterski J W, Ayala P Y, Morokuma K, Voth G A, Salvador P, Dannenberg J J, Zakrzewski V G, Dapprich S, Daniels A D, Strain M C, Farkas O, Malick D K, Rabuck A D, Raghavachari K, Foresman J B, Ortiz J V, Cui Q, Baboul A G, Clifford S, Cioslowski J, Stefanow B B, Liu G, Liashenko A, Piskorz P, Komaromi I, Martin R L, Fox D J, Keith T, Al-Laham M A, Peng C Y, Nanayakkara A, Challacombe M, Gill P M W, Johnson B, Chen W, Wong M W, Gonzalez C, Pople J A, *Gaussian 09 Revision*, (Gaussian Inc, Wallingford CT) 2004.
- Becke A D, *Phys Rev A*, 38 (1988) 3098.
- Lee C, Yang W & Parr R G, *Phys Rev B*, 37 (1988) 785.
- Frisch A, Nielsen A B & Holder A J, *Gauss View Users Manual*, (Gaussian Inc, Pittsburgh PA) 2000.
- Merrick J P, Moran D & Radom L, *J Phys Chem A*, 111 (2007) 11683.
- Ditchfield R, *J Chem Phys*, 56 (1972) 5688.
- Wolinski K, Hinton J F & Pulay P, *J Am Chem Soc*, 112 (1990) 8251.
- Tomasi J, Mennucci B & Cammi R, *Chem Rev*, 105 (2005) 2999.
- O'Boyle N M, Tenderholt A L & Langner K M, *J Comput Chem*, 29 (2008) 839.
- Scott A P & Radom L, *J Phys Chem*, 100 (1996) 16502.
- Yazıcı S, Albayrak Ç, Gümrükçüoğlu İ E, Şenel İ & Büyükgüngör O, *Spectrochim Acta A*, 93 (2012) 208.
- Reed A E, Curtiss L A & Weinhold F, *Chem Rev*, 88 (1988) 899.
- Mulliken R S, *J Chem Phys*, 23 (1955) 1841.
- Fleming J, *Frontier Orbitals and Organic Chemical Reactions*, (John Wiley & Sons Ltd, London) 1976.
- Diener M D & Alford J M, *Nature*, 393 (1998) 668.
- Yang S H, Pettiette C L, Conceicao J, Cheshnovsky O & Smalley R E, *Chem Phys Lett*, 139 (1987) 233.
- Handschuh H, Ganteför G, Kessler B, Bechthold P S & Eberhardt W, *Phys Rev Lett*, 74 (1995) 1095.
- Tanak H, Marchewka M K & Drozd M, *Spectrochim Acta A*, 105 (2013) 156.
- Gökçe H, Öztürk N, Ceylan Ü, Alpaslan Y B & Alpaslan G, *Spectrochim Acta A*, 163 (2016) 170.
- Durgun M, Ceylan Ü, Yalçın Ş P, Türkmen H, Özdemir N & Koyuncu İ, *J Mol Struct*, 1114 (2016) 95.
- Uzun S, Esen Z, Koç E, Usta N C & Ceylan M, *J Mol Struct*, 1178 (2019) 450.
- Chen M, Waghmare U V, Friend C M & Kaxiras E, *J Chem Phys*, 109 (1998) 6854.
- Köse E, Ataç A, Karabacak M, Nagabalasubramanian P B, Asiri A M & Periandy S, *Spectrochim Acta A*, 116 (2013) 622.
- Politzer P, Lane P & Murray J S, *Cent Eur J Energy Mater*, 8 (2011) 39.

- 29 Saka E T, Uzun S & Çağlar Y, *J Organomet Chem*, 810 (2016) 25.
- 30 Thanthiriwatte K S & Nalin de Silva K M, *J Mol Struct*, 617 (2002) 169.
- 31 Asiri A M, Karabacak M, Kurt M & Alamry K A, *Spectrochim Acta A*, 82 (2011) 444.
- 32 Zacharias A O, Varghese A, Akshaya K B, Savitha M S & George L, *J Mol Struct*, 1158 (2018) 1.
- 33 Morell C, Grand A & Toro-Labbé A, *J Phys Chem A*, 109 (2005) 205.
- 34 Singh R N, Kumar A, Tiwari R K, Rawat P, Verma D & Baboo V, *J Mol Struct*, 1016 (2012) 97.
- 35 Demircioğlu Z, Ersanlı C C, Kantar G K & Şaşmaz S, *J Mol Struct*, 1181 (2019) 25.
- 36 Uzun S, Demircioğlu Z, Taşdoğan M & Ağar E, *J Mol Struct*, 1206 (2020) Article 127749.